

---

# Recent results from NNLOJET

Nigel Glover

IPPP, Durham University

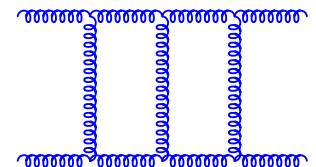
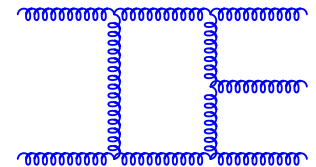
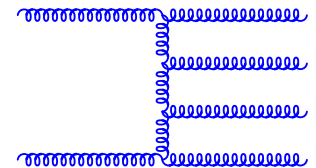


HiggsTools Third Annual Meeting  
Torino, 15 May 2017

# Anatomy of a Higher Order calculation

e.g. pp to JJ at NNLO

- ✓ double real radiation matrix elements  $d\hat{\sigma}_{NNLO}^{RR}$ 
  - ✚ implicit poles from double unresolved emission
- ✓ single radiation one-loop matrix elements  $d\hat{\sigma}_{NNLO}^{RV}$ 
  - ✚ explicit infrared poles from loop integral
  - ✚ implicit poles from soft/collinear emission
- ✓ two-loop matrix elements  $d\hat{\sigma}_{NNLO}^{VV}$ 
  - ✚ explicit infrared poles from loop integral



$$d\hat{\sigma}_{NNLO} \sim \int_{d\Phi_{m+2}} d\hat{\sigma}_{NNLO}^{RR} + \int_{d\Phi_{m+1}} d\hat{\sigma}_{NNLO}^{RV} + \int_{d\Phi_m} d\hat{\sigma}_{NNLO}^{VV}$$

# Anatomy of a Higher Order calculation

e.g. pp to JJ at NNLO

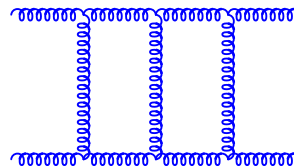
- ✓ Double real and real-virtual contributions used in NLO calculation of  $X+1$  jet



Can exploit NLO automation

... but needs to be evaluated in regions of phase space where extra jet is not resolved

- + Two loop amplitudes - very limited set known



... currently far from automation

- + Method for cancelling explicit and implicit IR poles - overlapping divergences

... currently not automated

# NNLOJET

X. Chen, J. Cruz-Martinez, J. Currie, A. Gehrmann-De Ridder, T. Gehrmann, NG, A. Huss, M. Jaquier, T. Morgan, J. Niehues, J. Pires

Implementing NNLO corrections including decays for

- ✓  $pp \rightarrow H, W, Z$
- ✓  $pp \rightarrow H + J$  1408.5325, 1607.08817
- ✓  $pp \rightarrow Z + J$  1507.02850, 1605.04295, 1610.01843
- ✓  $pp \rightarrow JJ$  1301.7310, 1310.3993, 1611.01460, 1704.00923
- ✓  $ep \rightarrow JJ + (J)$  1606.03991, 1703.05977
- ✓ ...

using Antenna subtraction

$$|M(1, \dots, i, j, k, \dots, n)|^2 \rightarrow X(i, j, k) |M(1, \dots, I, K, \dots, n)|^2$$

- ✓ all singularities associated with  $j$  soft or collinear with  $i$  or  $k$  are concentrated in antenna  $X$
- ✓  $I$  and  $K$  are resolved partons

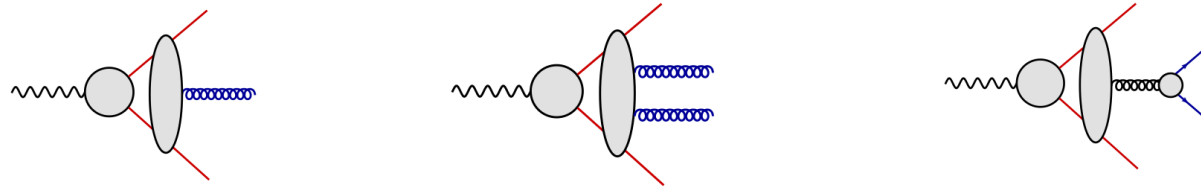
# Antenna subtraction at NNLO

- ✓ Antenna subtraction exploits the fact that matrix elements already possess the intricate overlapping divergences

$$X_3^0(i, j, k) \sim \frac{|\mathcal{M}_3^0(i, j, k)|^2}{|\mathcal{M}_2^0(I, K)|^2}, \quad X_4^0(i, j, k, l) \sim \frac{|\mathcal{M}_4^0(i, j, k, l)|^2}{|\mathcal{M}_2^0(I, L)|^2}$$

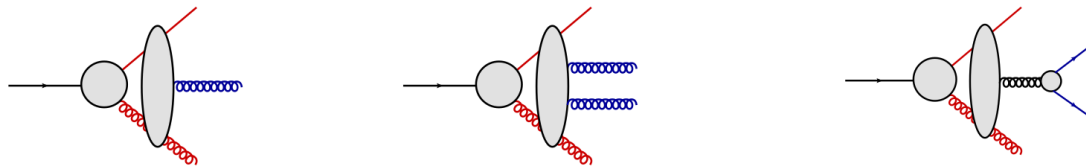
Quark-antiquark:

$$\gamma^* \rightarrow q\bar{q} + \dots$$



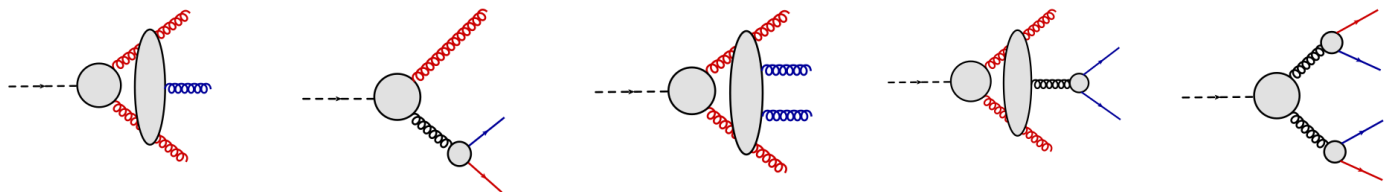
Quark-gluon:

$$\bar{\chi}^0 \rightarrow \tilde{g}g + \dots$$



Gluon-gluon:

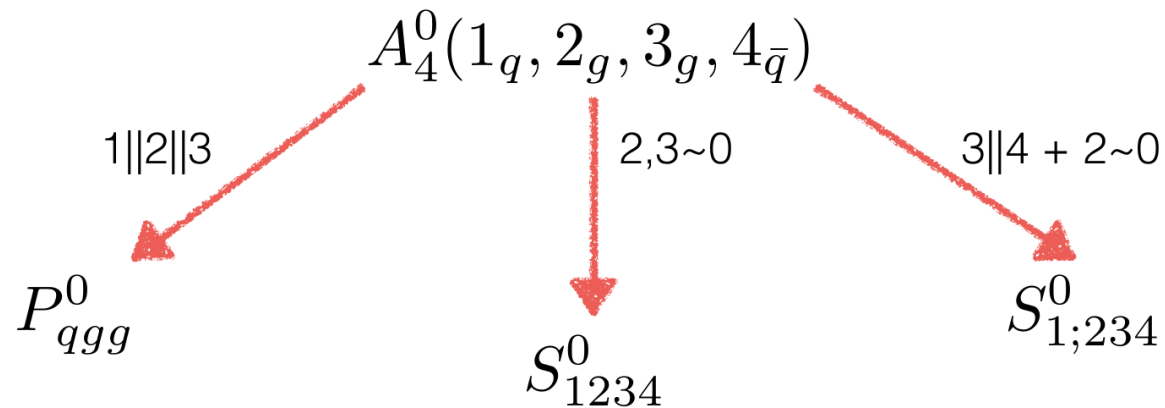
$$H \rightarrow gg + \dots$$



- ✓ plus mappings  $i + j + k \rightarrow I + J, i + j + k + l \rightarrow I + L$

# Antenna subtraction at NNLO

- ✓ Antenna mimics all singularities of QCD

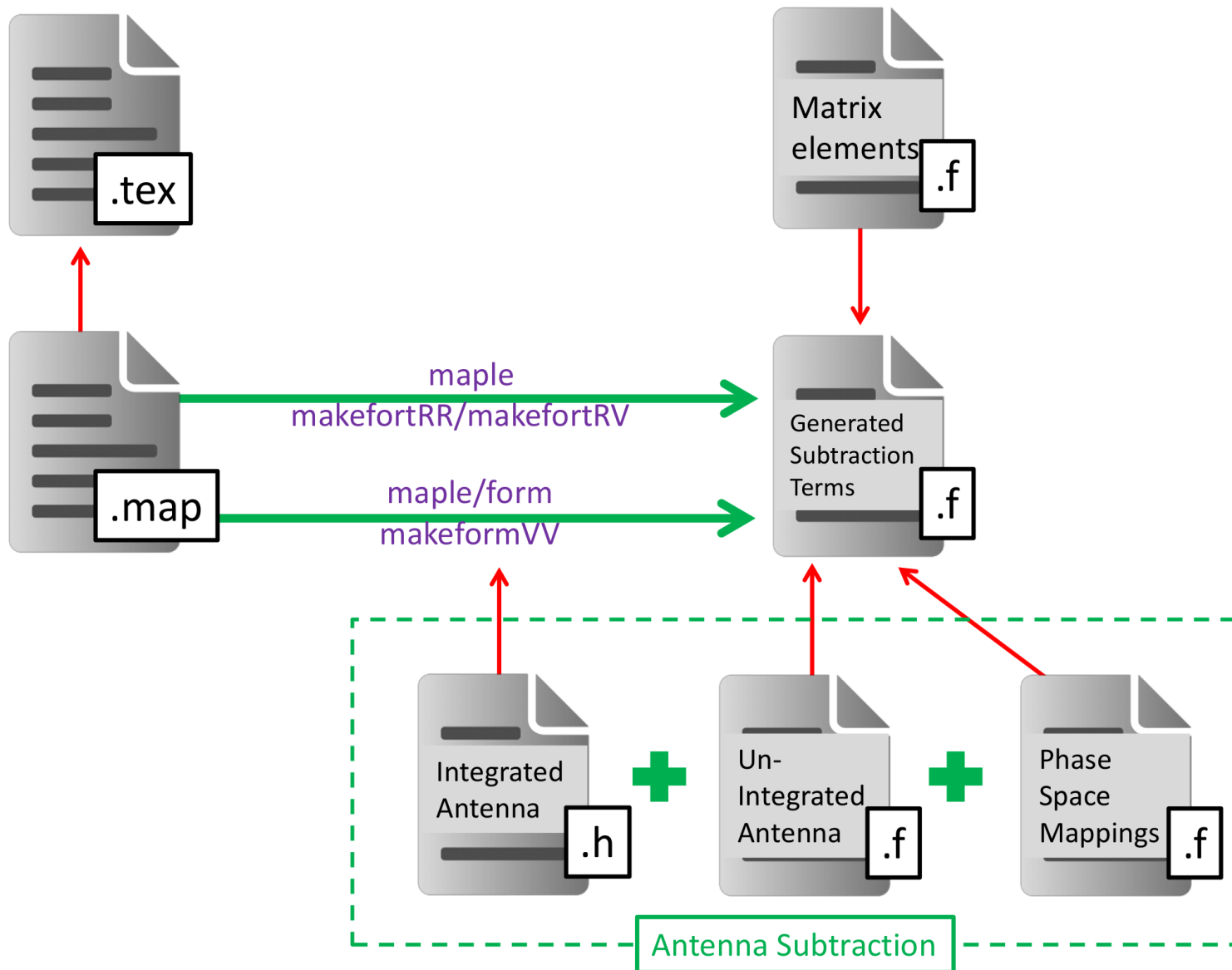


- ✓ Phase space map smoothly interpolates momenta for reduced matrix element between limits

$$\widetilde{(123)} = xp_1 + r_1p_2 + r_2p_3 + zp_4$$

$$\widetilde{(234)} = (1-x)p_1 + (1-r_1)p_2 + (1-r_2)p_3 + (1-z)p_4$$

# Automatically generating the code (1)



# Maple script: RR example



```
+F40a(i, j, k, l) *A4g0(1, 2, [i, j, k], [j, k, l])  
-f30FF(i, j, k) *f30FF([i, j], [j, k], l)  
*A4g0(1, 2, [[i, j], [j, k]], [[j, k], l])
```

...

```
+F4^{0,a}(i, j, k, l) A4^0(1, 2, (\widetilde{ijk}), (\widetilde{jkl}))
```

```
-f3^0(i, j, k) f3^0((\widetilde{ij}), (\widetilde{jk}), l) A4^0(1, 2, [(\widetilde{ij}), (\widetilde{jk})], ((\widetilde{jk})l))
```

...

✓  $X_4^0, X_3^0$  (and  $X_3^1$  in RV) are unintegrated antennae

✓  $[i, j, k]$  or  $(\widetilde{ijk})$  are mapped momenta



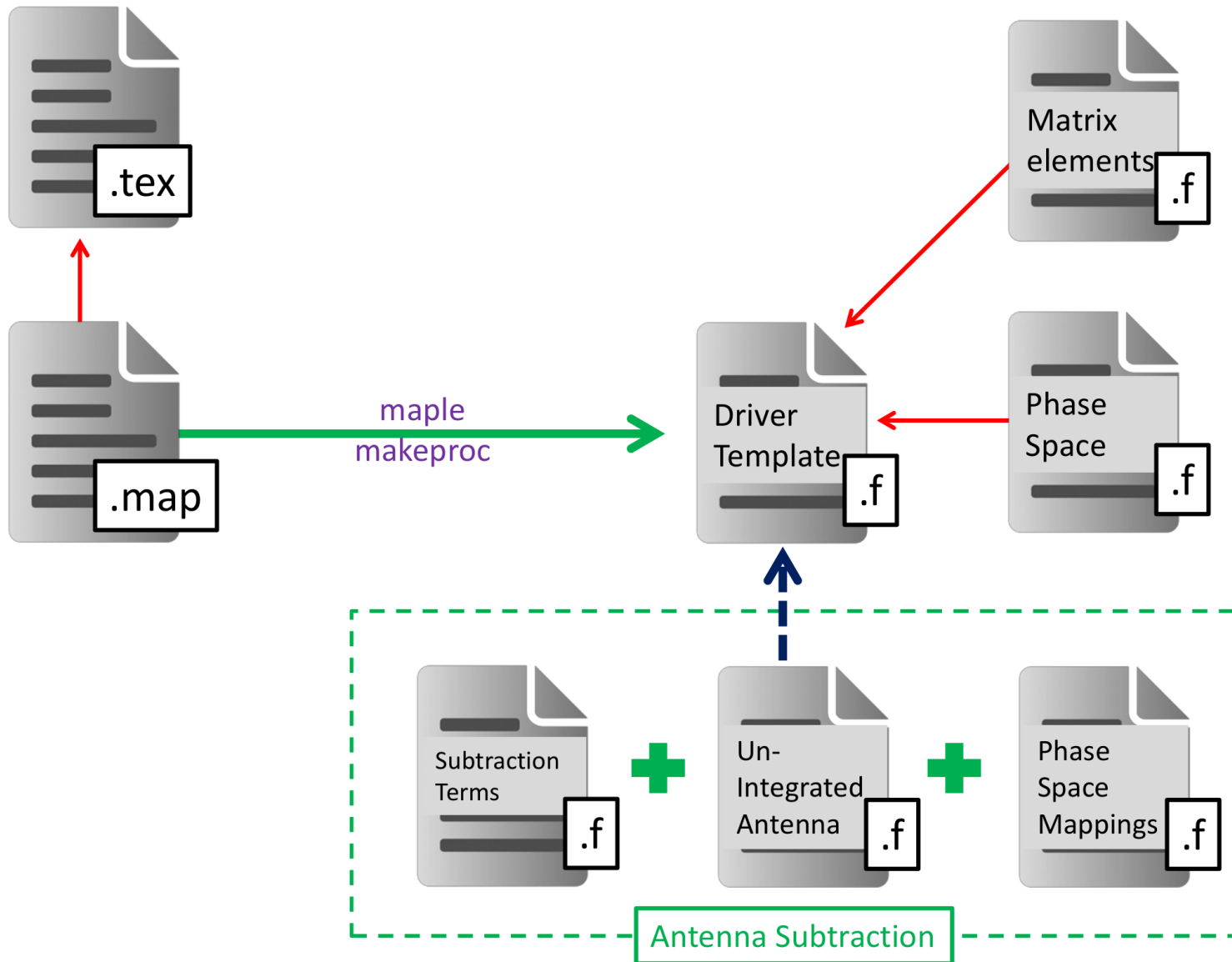
# Maple script: VV example



$$\begin{aligned}
 & - (+1/2 * \text{calgF40FI}(2, 3) \\
 & + 1/2 * \text{calgF31FI}(2, 3) \\
 & + b_0/e * 1/2 * \text{QQ}(s_{23}) * \text{calgF30FI}(2, 3) \\
 & - b_0/e * 1/2 * \text{calgF30FI}(2, 3) \\
 & - 1/2 * \text{calgF30FI}(2, 3) * 1/2 * \text{calgF30FI}(2, 3) \\
 & - 1/2 * \text{gamma2gg}(z_2) \\
 & + b_0/e * 1/2 * \text{gamma1gg}(z_2) \\
 & ) * A_4 g_0(1, 2, 3, 4) \\
 & \dots
 \end{aligned}
 + \left[ \begin{aligned}
 & - \frac{1}{2} \mathcal{F}_{4,g}^0(s_{23}) \\
 & - \frac{1}{2} \mathcal{F}_{3,g}^1(s_{23}) \\
 & - \frac{b_0}{2\epsilon} \left( \frac{s_{23}}{\mu_R^2} \right)^{-\epsilon} \mathcal{F}_{3,g}^0(s_{23}) \\
 & + \frac{b_0}{2\epsilon} \mathcal{F}_{3,g}^0(s_{23}) \\
 & + \frac{1}{4} \mathcal{F}_{3,g}^0(s_{23}) \otimes \mathcal{F}_{3,g}^0(s_{23}) \\
 & + \frac{1}{2} \Gamma_{gg}^{(2)}(z_2)
 \end{aligned} \right]$$

✓  $\mathcal{X}_4^0$ ,  $\mathcal{X}_3^0$  and  $\mathcal{X}_3^1$  are integrated antennae

# Automatically generating the code (2)



# Maple script to produce driver template



```
R := [
  [A5g0, [g, g, g, g, g], 1],
  [B3g0, [qb, g, g, g, q], 1/nc],
  ...
]:
```

$$d\sigma_{gg}^R = \mathcal{N}_{LO} \left( \frac{\alpha_s N}{2\pi} \right) \left[ \begin{aligned} &+ 2 \frac{1}{3!} \left( \sum_{12} A5g0(1, 2, 3, 4, 5) - \text{ggA5g0SNLO}(1, 2, 3, 4, 5) \right) \\ &+ \frac{N_F}{N} \left( \sum_6 B3g0(3, 1, 2, 4, 5) - \text{ggB3g0SNLO}(3, 1, 2, 4, 5) \right) \\ &\dots \end{aligned} \right]$$

# Checks

- ✓ Analytic pole cancellations for RV, VV ✓ Unresolved limits for RR, RV

$$\text{Poles} \left( d\sigma^{RV} - d\sigma^T \right) = 0$$

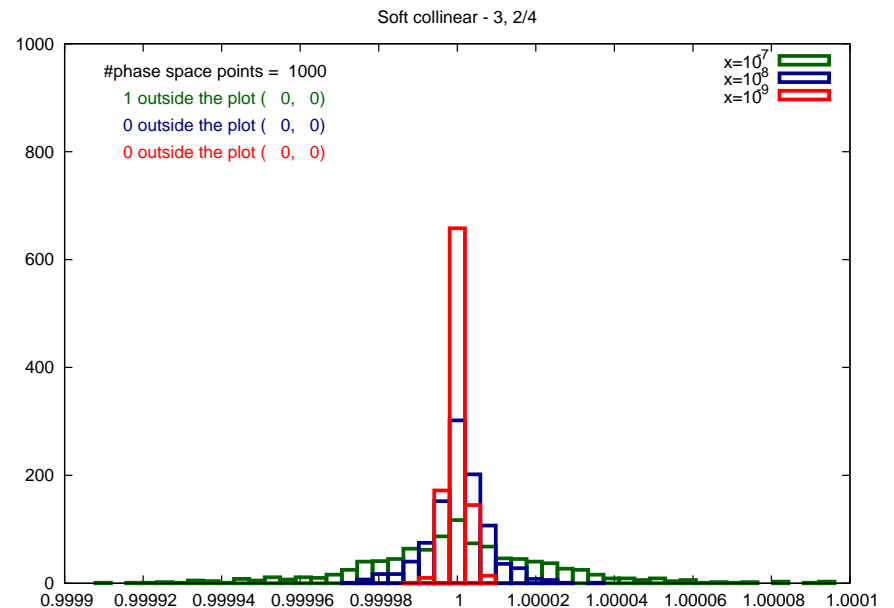
$$\text{Poles} \left( d\sigma^{VV} - d\sigma^U \right) = 0$$

$$d\sigma^S \longrightarrow d\sigma^{RR}$$

$$d\sigma^T \longrightarrow d\sigma^{RV}$$

$$q\bar{q} \rightarrow Z + g_3 g_4 g_5 \text{ (} g_3 \text{ soft \& } g_4 \parallel \bar{q} \text{)}$$

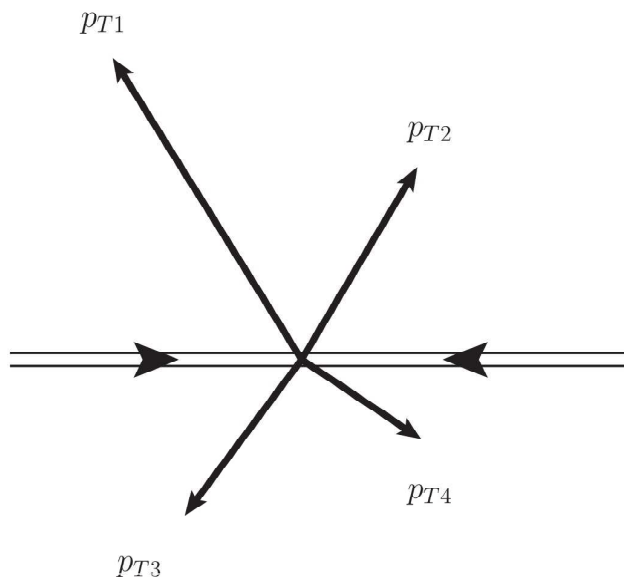
```
09:26:35 ..maple/process/Z
$ form autoqgB1g2ZgtoqU.frm
FORM 4.1 (Mar 13 2014) 64-bits
#-
poles = 0;
6.58 sec out of 6.64 sec
```



# Single Jet Inclusive Distribution

Currie, NG, Pires (16)

- ✓ Classic jet observable



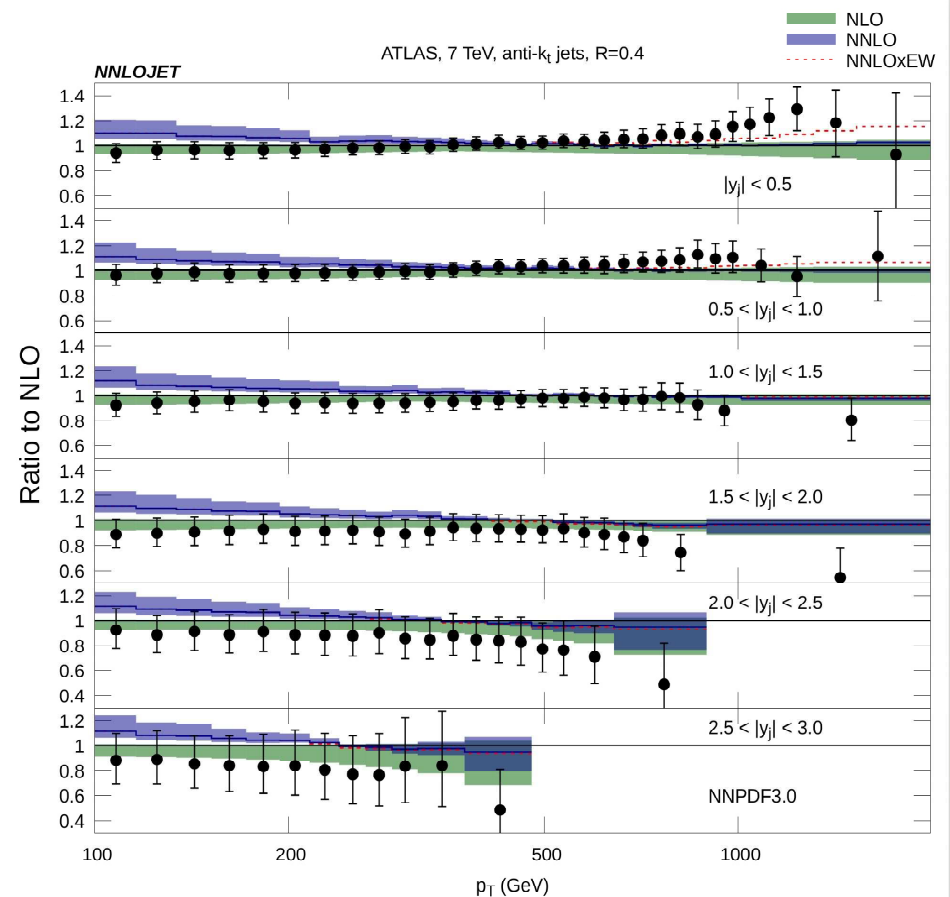
- ✓ Every jet in the event enters in the distribution
- ✓ Expect sensitivity to PDFs
- ✓ ... and to  $\alpha_s$

- ✓ All sub-processes included  
–  $gg, gq, q\bar{q}, qq$  etc
- ✓ in leading colour approximation  
i.e. all  $\alpha_s^2 N^2, \alpha_s^2 N N_F, \alpha_s^2 N_F^2$   
contributions relative to Born
- ✗ missing corrections  
 $O(1), N_F/N, 1/N^2, N_F/N^3, 1/N^4$
- ✓ expect to be less than 10% of the NNLO correction (as at NLO)

# Single Jet Inclusive Distribution – $R=0.4$

Currie, NG, Pires (16)

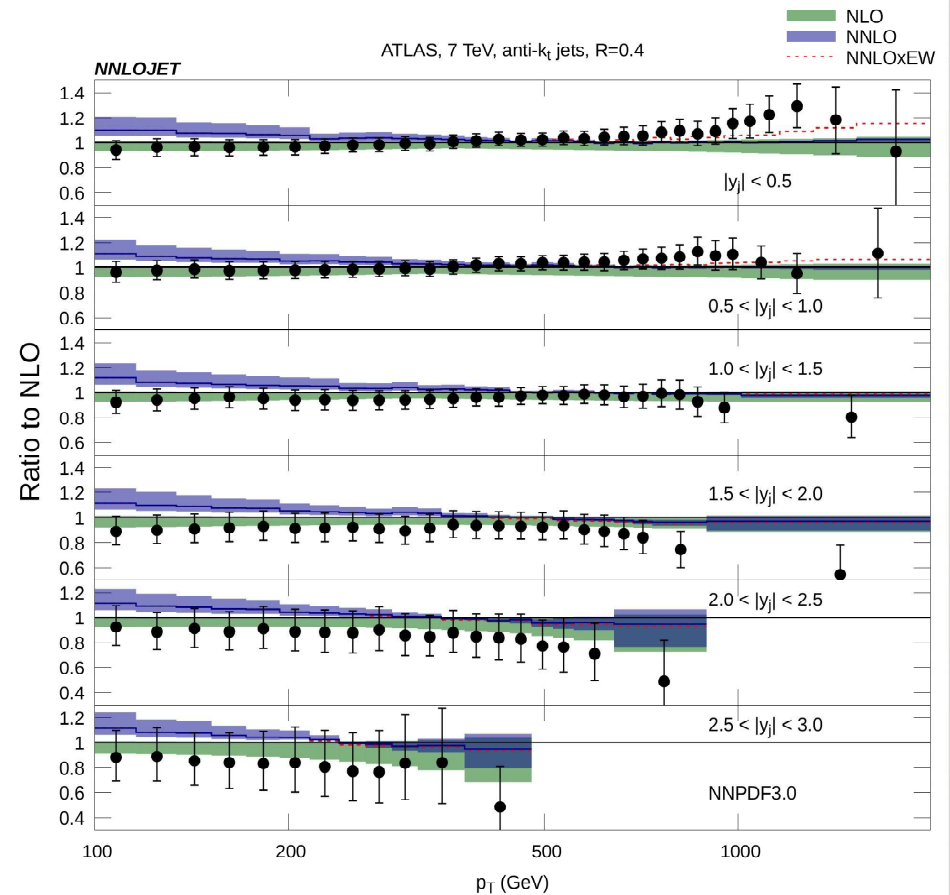
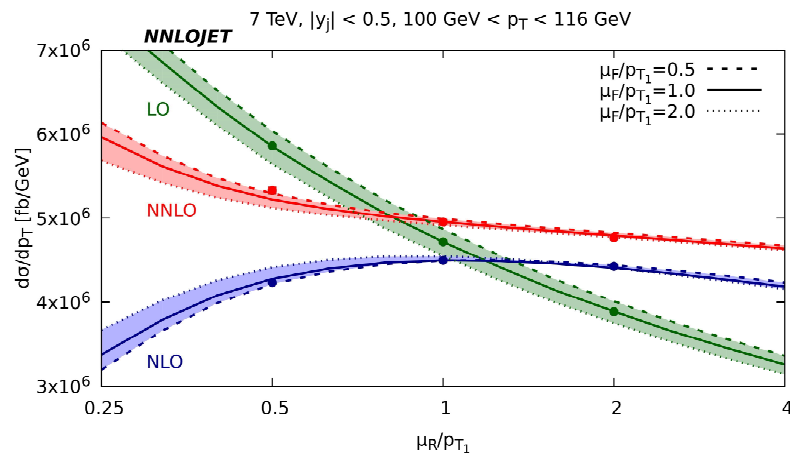
- ✓ ATLAS 7 TeV data,  $4.5 \text{ fb}^{-1}$   
JHEP02(2015)153  
JHEP09(2015)141 (Erratum)
- ✓ anti- $k_T$  algorithm with  $R = 0.4$
- ✓ six rapidity slices,  
 $0 - 0.5$ ,  $0.5 - 1.0$ ,  $1.0 - 1.5$ ,  $1.5 - 2.0$ ,  
 $2.0 - 2.5$ ,  $2.5 - 3.0$
- ✓ NNPDF3.0\_NNLO PDFs
- ✓ negligible NP corrections



# Single Jet Inclusive Distribution – R=0.4

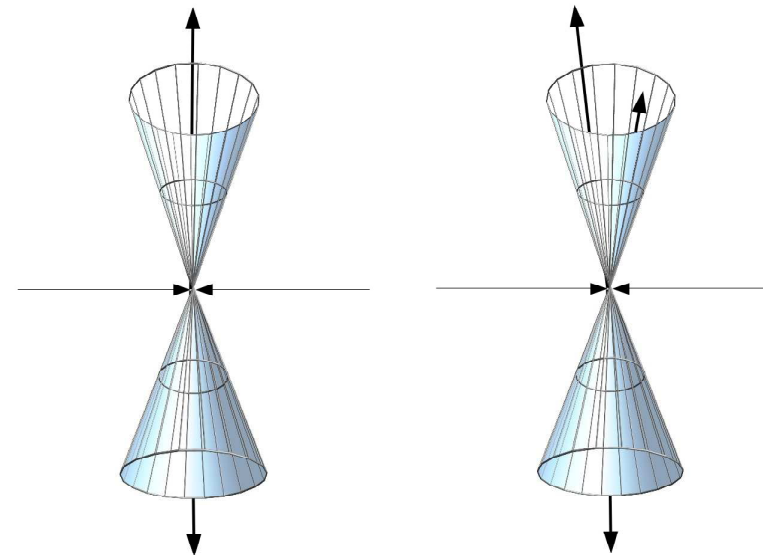
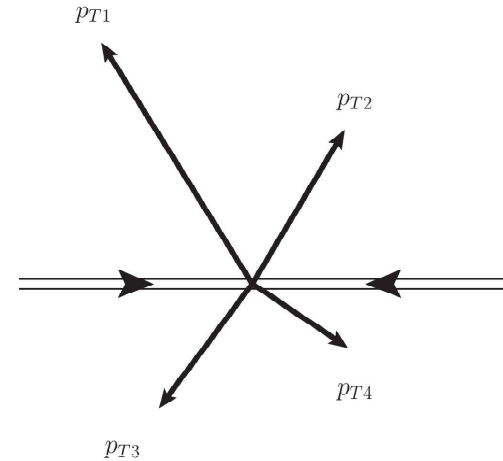
Currie, NG, Pires (16)

- ✓ NLO describes the data pretty well
- ✓ NLO has relatively small scale dependence
  - because the central scale choice lies close to the turning point in the scale variation plot
- ✓ NNLO effects around 10% at low  $p_T$  and small at high  $p_T$



# Scale Choice

- ✓ no fixed hard scale for jet production
- ✓ two widely used scale choices
  - ➡ leading jet  $p_T$  ( $p_{T1}$ )
  - ➡ individual jet  $p_T$  ( $p_T$ )
- ✓ different scale changes PDF and  $\alpha_s$
- ✓ no difference for back-to-back jet configurations (only arises at higher orders)

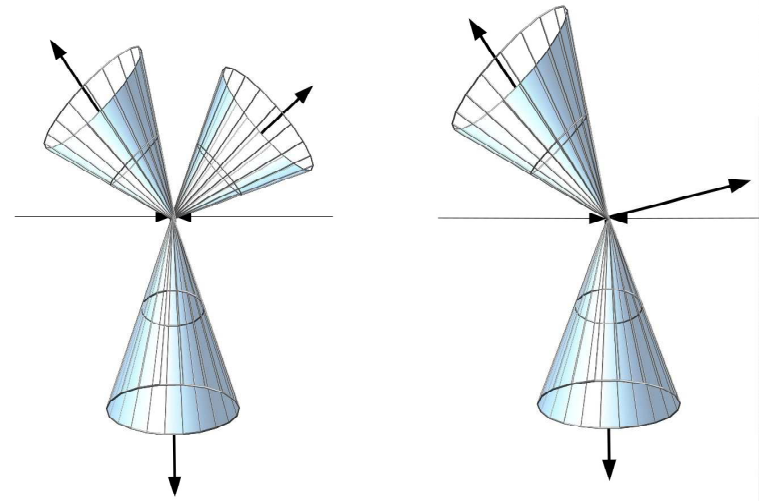




# Scale Choice

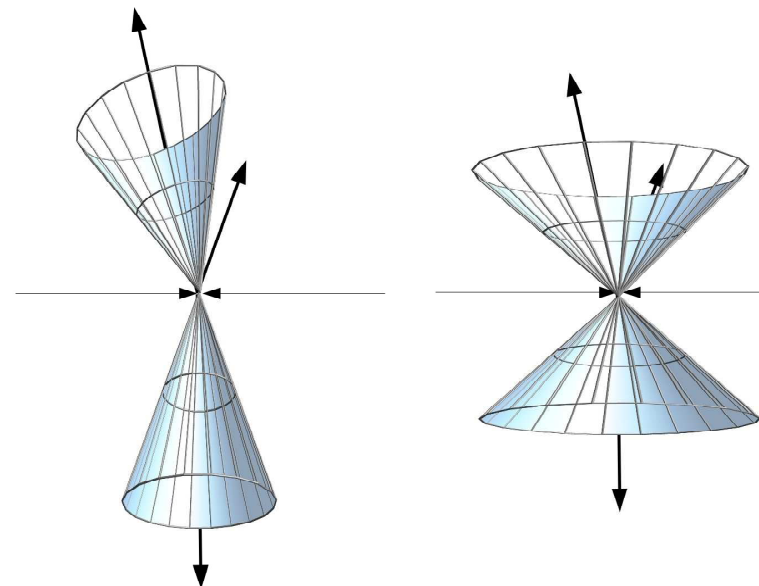
At NLO,  $p_T \neq p_{T1}$  for

- ✓ 3-jet rate (small effect)
- ✓ 2-jet rate (3rd parton falls outside jet)

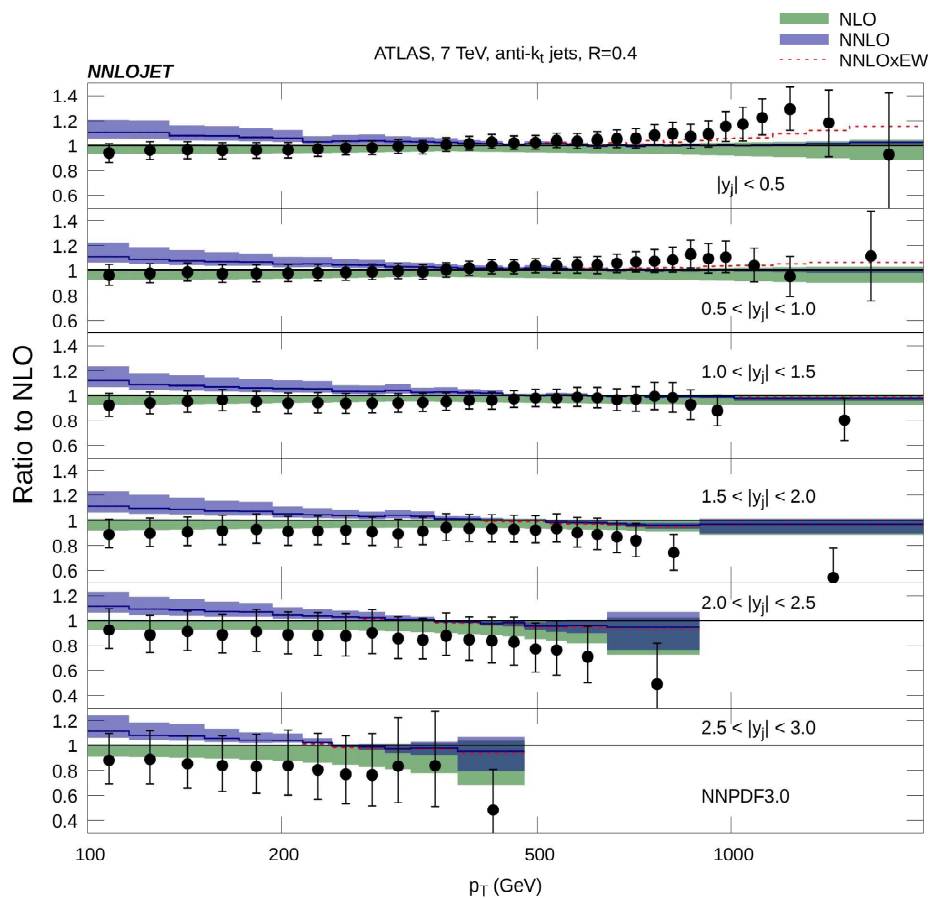


Changing  $R$  has an effect on the cross section, but also on the scale choice:

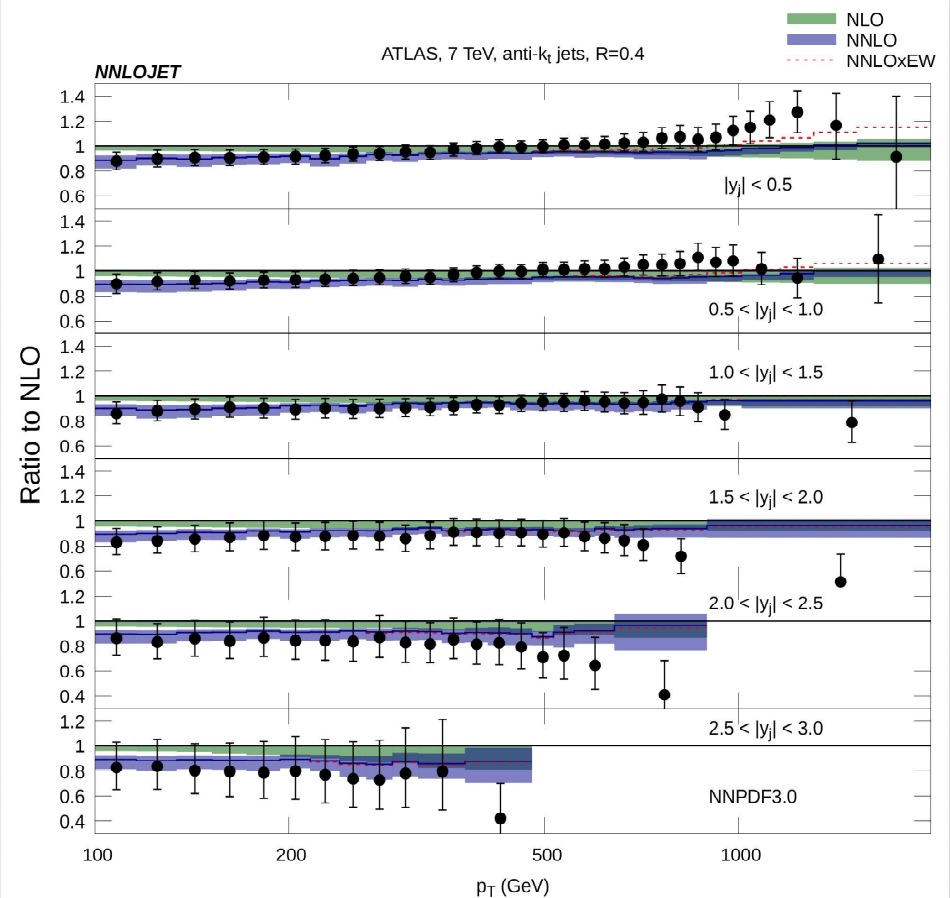
- ✓ introduces spurious  $R$ -dependence in scale choice
- ✓  $p_{T1}$  scale has no  $R$ -dependence at NLO, unlike  $p_T$
- ✓ at NNLO  $p_{T1}$  scale depends on  $R$  in some four-parton configurations



# Single Jet Inclusive Distribution – R=0.4



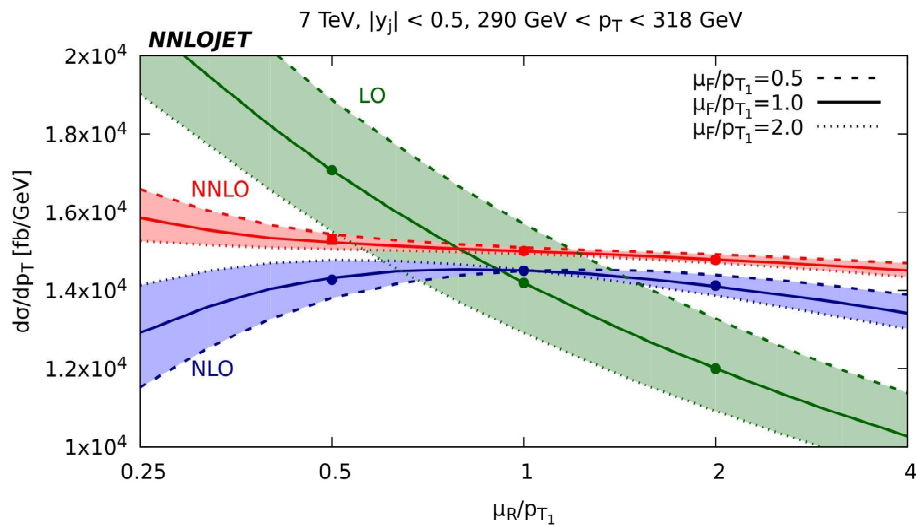
$$\mu_R = \mu_F = p_{T1}$$



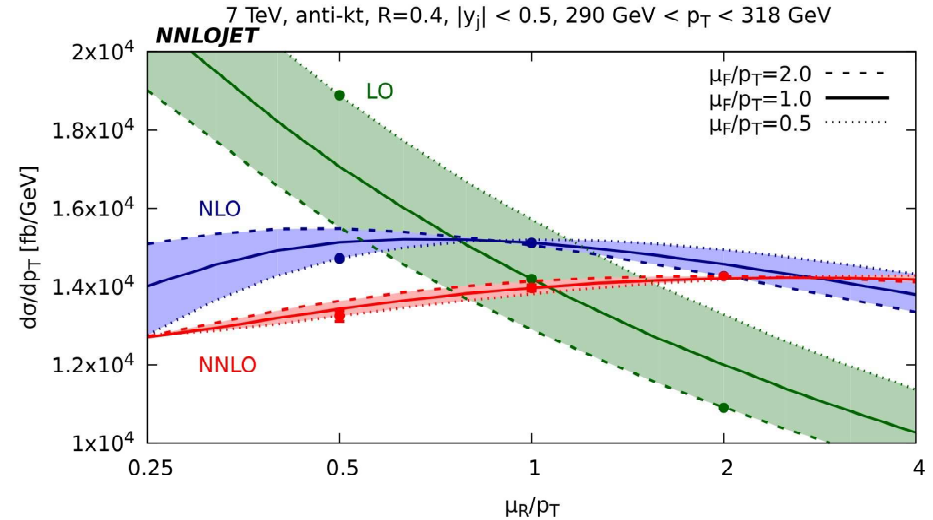
$$\mu_R = \mu_F = p_T$$

- ✗ Quite different behaviour!
- ✓ NLO with  $\mu = p_{T1}$  describes  $R = 0.4$  data quite well
- ✓ NNLO with  $\mu = p_T$  describes  $R = 0.4$  data quite well

# Single Jet Inclusive Distribution – R=0.4



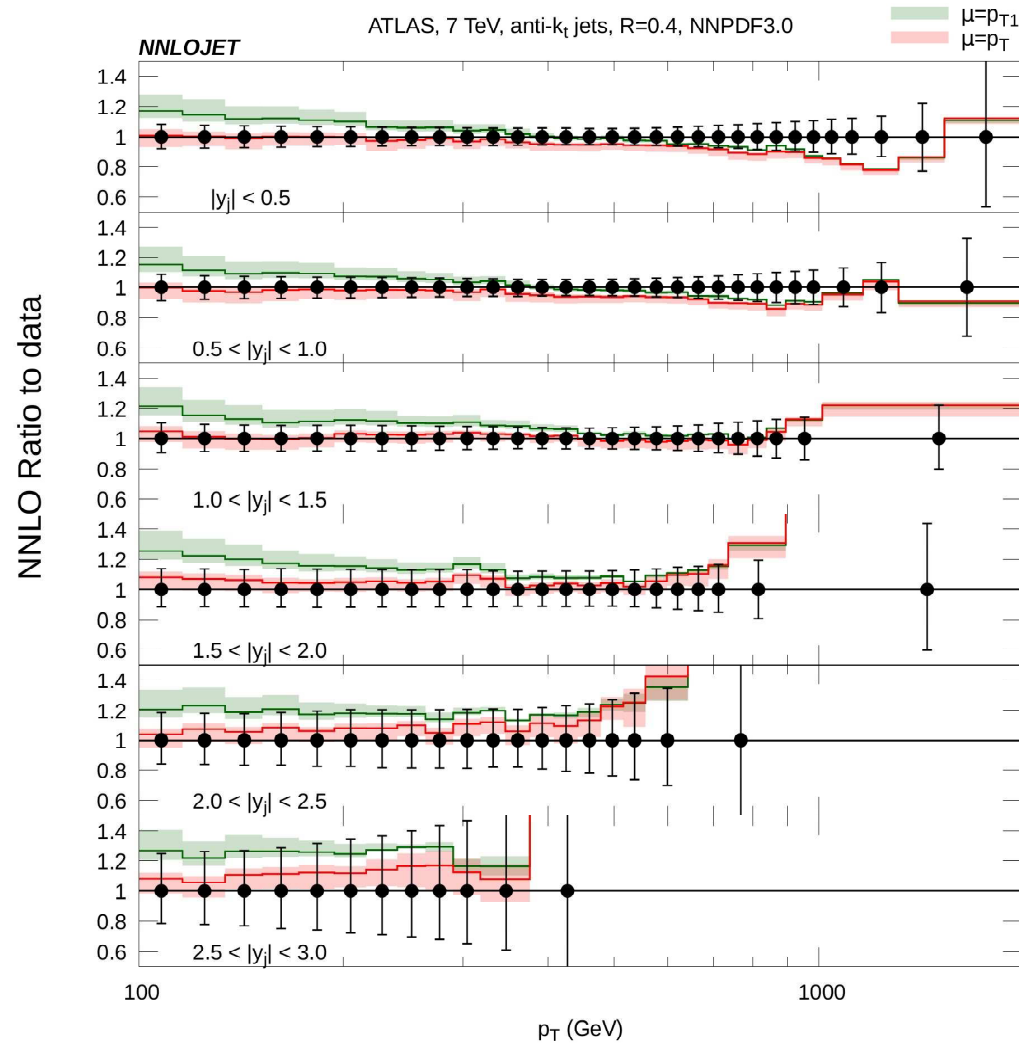
$$\mu_R = \mu_F = p_{T1}$$



$$\mu_R = \mu_F = p_T$$

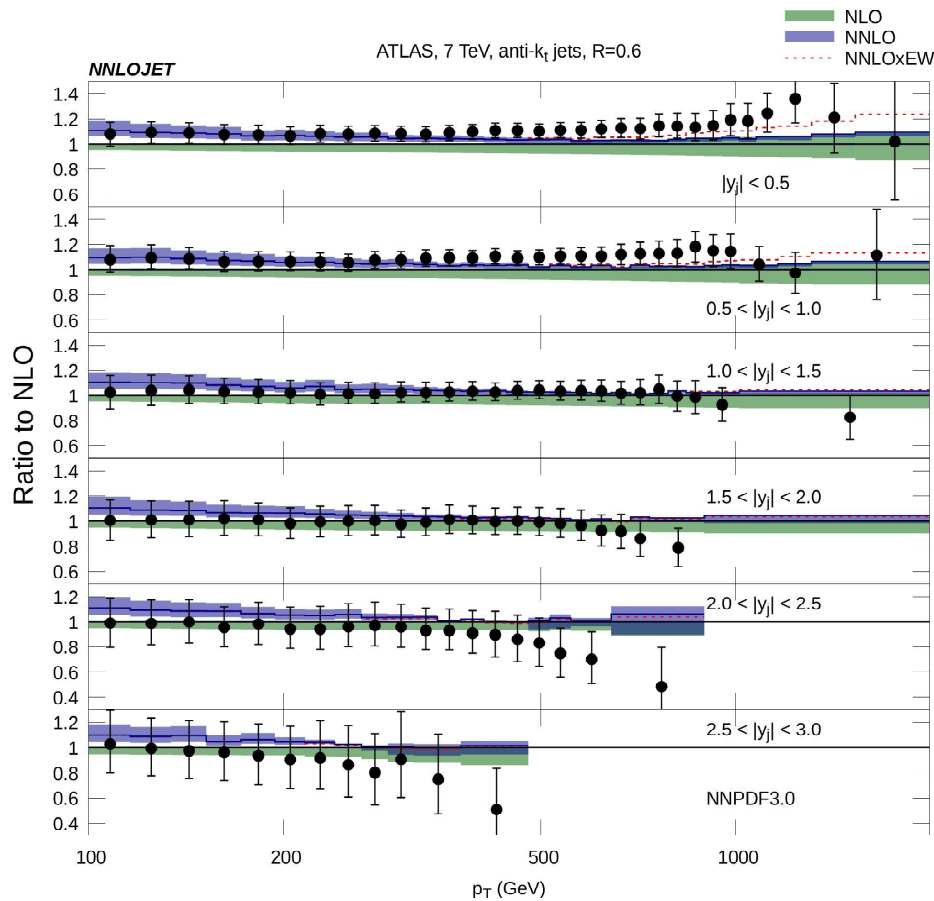
- ✗ Quite different behaviour!
- ➡ scale uncertainty much smaller than difference between scale choices
- ➡ explore alternative scale choices

# Single Jet Inclusive Distribution – R=0.4

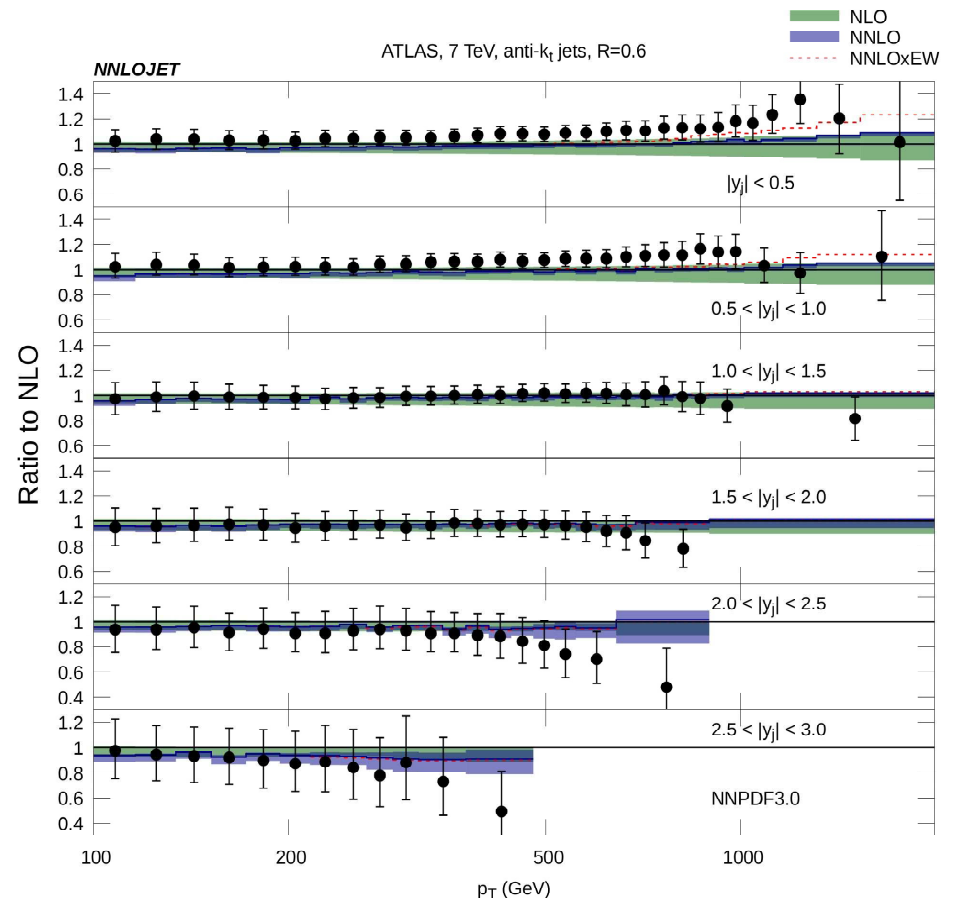


✗ Scale uncertainty is smaller than the uncertainty in choosing  $p_T$  or  $p_{T1}$

# Single Jet Inclusive Distribution – R=0.6



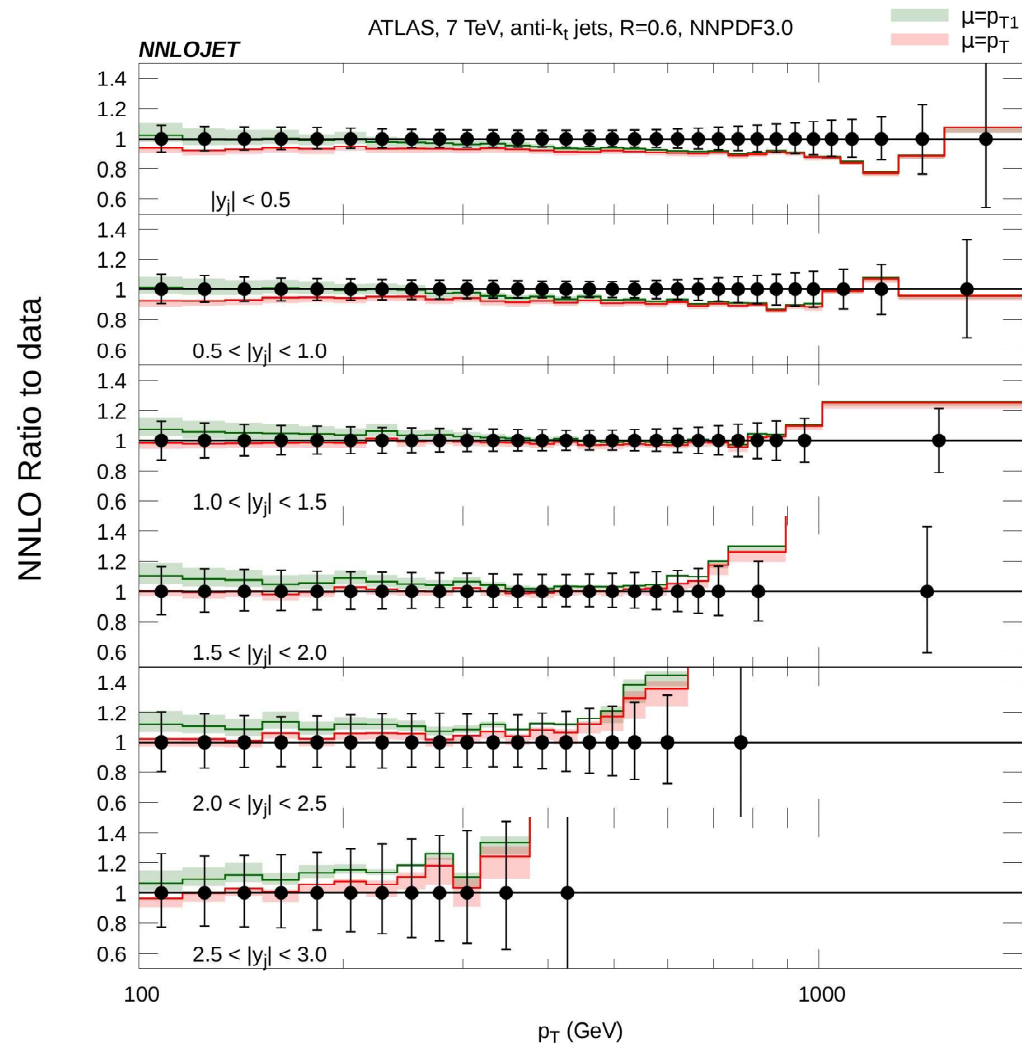
$$\mu_R = \mu_F = p_{T1}$$



$$\mu_R = \mu_F = p_T$$

- ✗ Quite different behaviour!
- ✓ NLO with  $\mu = p_T$  describes  $R = 0.6$  data quite well
- ✓ NNLO with  $\mu = p_{T1}$  describes  $R = 0.6$  data quite well

# Single Jet Inclusive Distribution – R=0.6



✗ Scale uncertainty is smaller than the uncertainty in choosing  $p_T$  or  $p_{T1}$

# CPU cost

✓ Standalone production run with fixed  $\sqrt{s}$ , fixed  $R$ , fixed PDF, three scale variation for  $\mu = p_{T1}$  and  $\mu = p_T$  (Warmup  $\sim 1-2\%$ )

Job Type	No. Jobs	Runtime/Job (hr)	Total Runtime
LO	200	0.5	100
NLO-V	500	1.5	750
NLO-R	500	2	1000
NNLO-VV	600	20	12000
NNLO-RV	2500	50	125000
NNLO-RRa	3500	50	175000
NNLO-RRb	2000	20	40000
			<b>353850</b>

✓ because LO is independent of  $R$  and  $p_T = p_{T1}$  to obtain different cone sizes/different scales can do a (much cheaper) NLO 3-jet calculation

$$\begin{aligned} \frac{d\sigma^{NNLO}(R_2)}{dp_T} &= \frac{d\sigma^{NNLO}(R_1)}{dp_T} + \left( \frac{d\sigma^R(R_2)}{dp_T} - \frac{d\sigma^R(R_1)}{dp_T} \right) \\ &+ \left( \frac{d\sigma^{RV}(R_2)}{dp_T} - \frac{d\sigma^{RV}(R_1)}{dp_T} \right) + \left( \frac{d\sigma^{RR}(R_2)}{dp_T} - \frac{d\sigma^{RR}(R_1)}{dp_T} \right) \end{aligned}$$

# Summary

- + NNLOJET is able to make a range of fully differential parton level NNLO predictions that can be compared with LHC fiducial cross sections
- code is partially automated and typically requires significant CPU resource
- need validation with different IR subtraction schemes
- + results show anticipated features of NNLO calculations - reduction of scale uncertainty, stabilisation of perturbative series, etc
- serious study of choice of scales and pdf uncertainties needed and in progress
- ✓ Single jet inclusive distribution
  - + Reduction of the scale uncertainty but ...
  - difference between common scale choices  $p_T$  and  $p_{T1}$  larger than scale uncertainty
  - + NP effects important at large  $R$ , low  $p_T$  ( $\sim 30\%$  for  $R = 0.7$ ,  $p_T \sim 50$  GeV)
  - + EW effects important at large  $p_T$  ( $\sim 5\%$  for  $p_T \sim 1000$  GeV)

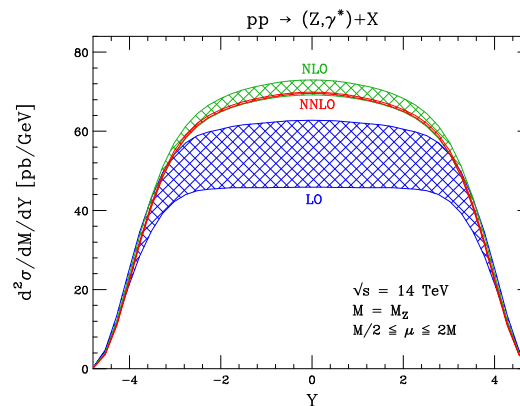
## Work in progress:

- ✓ Including other processes, such as dijets, other Higgs decays, etc
- ✓ Studying potential of data to constrain PDF sets and interface to APPLgrid, fastNLO

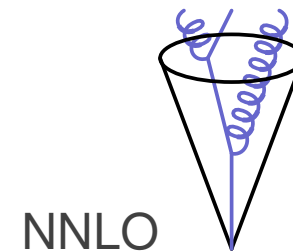
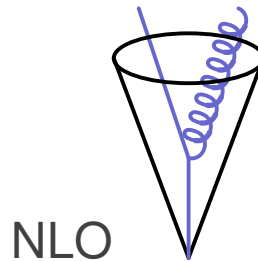
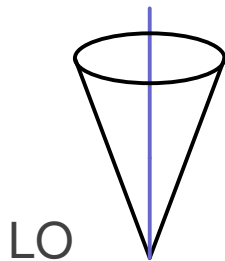


# What to expect from NNLO (1)

- ✓ Reduced renormalisation scale dependence



- ✓ Better able to judge convergence of perturbation series
- ✓ Fiducial (parton level) cross sections. Fully differential, so that experimental cuts can be applied directly
- ✓ Event has more partons in the final state so perturbation theory can start to reconstruct the shower
  - ➡ better matching of jet algorithm between theory and experiment

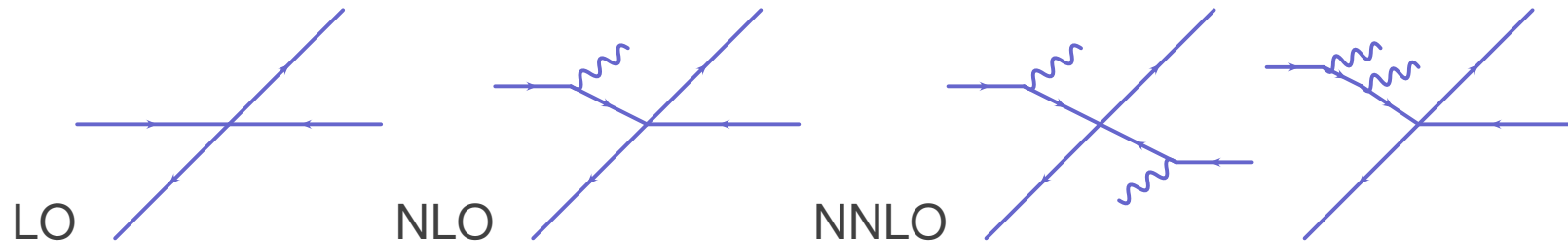


# What to expect from NNLO (2)

- ✓ All channels present at NNLO

LO	NLO	NNLO
gg	gg, qg	gg, qg, qq
q $\bar{q}$	q $\bar{q}$ , qg	q $\bar{q}$ , qg, gg

- ✓ Better description of transverse momentum of final state due to double radiation off initial state



- ✓ At LO, final state has no transverse momentum
- ✓ Single hard radiation gives final state transverse momentum, even if no additional jet
- ✓ Double radiation on one side, or single radiation of each incoming particle gives more complicated transverse momentum to final state